iScience, Volume *23*

Supplemental Information

Exposure to Air Pollution Disrupts Circadian Rhythm through Alterations in Chromatin Dynamics

Rengasamy Palanivel, Vinesh Vinayachandran, Shyam Biswal, Jeffrey A. Deiuliis, Roshan Padmanabhan, Bongsoo Park, Roopesh Singh Gangwar, Jared C. Durieux, Elaine Ann Ebreo Cara, Lopa Das, Graham Bevan, Zahi A. Fayad, Ahmed Tawakol, Mukesh K. Jain, Sujata Rao, and Sanjay Rajagopalan

Supplemental Documents

Supplementary Figure 1

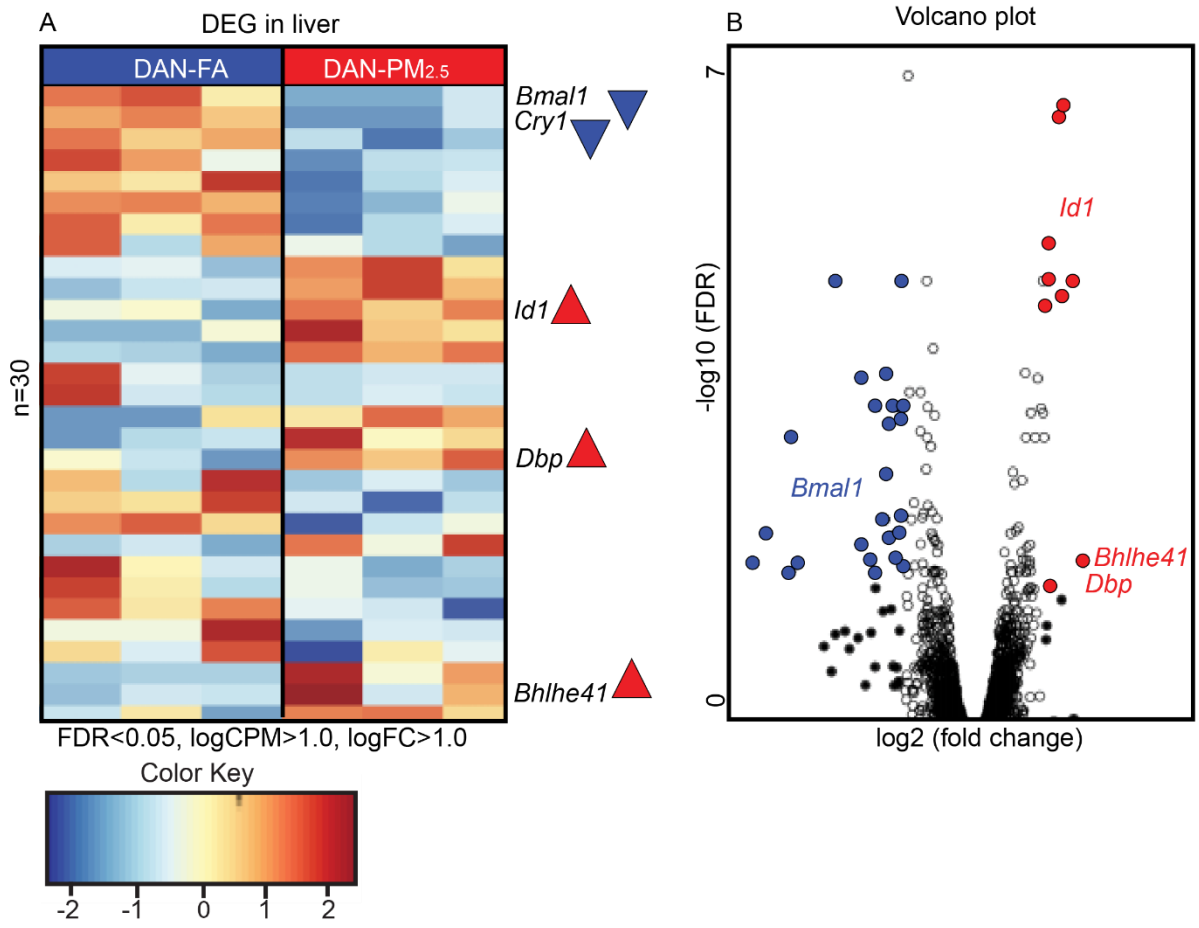

Figure S1. Unbiased transcriptomic analysis of liver samples (ZT02) in mice exposed to $PM_{2.5}$ for 14 weeks, Related to Figure 1

Supplementary Figure 2

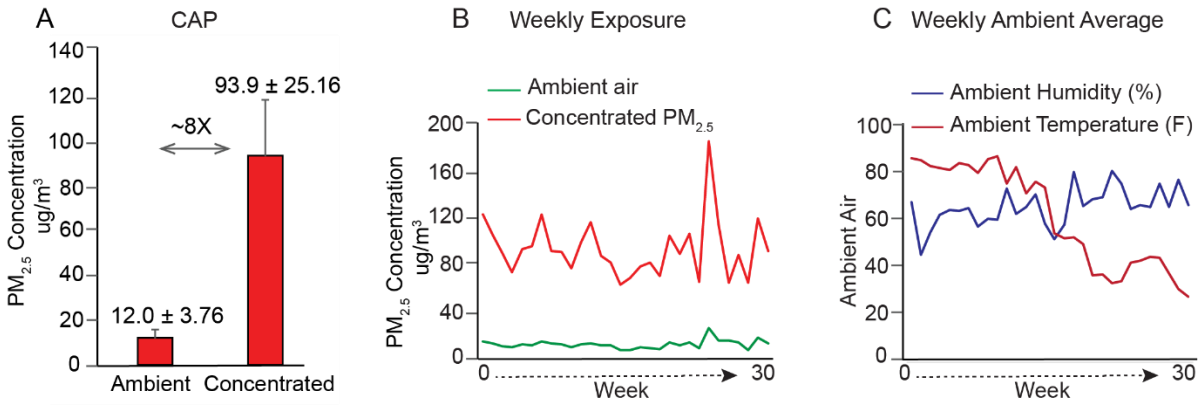

D Level of Elemental Concentration in Ambient vs Concentrated air (Air pollution)

Elements	Ambient Air (ng/cm²) Mean ± SD	Concentrated $PM_{2.5}$ (ng/cm²) Mean ± SD
Na	349.96 ± 39.48	712.98 ± 252.36
Mg	76.31 ± 13.94	187.32 ± 73.29
Al	50.66 ± 37.95	225.38 ± 235.58
Si	37.77 ± 72.68	577.72 ± 506.55
S	75.48 ± 209.77	1870.92 ± 1016.83
Cl	4.37 ± 6.40	10.05 ± 59.99
K	10.75 ± 19.11	176.87 ± 93.36
Ca	34.91 ± 56.82	508.05 ± 412.04
Ti	4.74 ± 3.19	31.94 ± 21.98
Fe	40.84 ± 60.47	736.86 ± 527.86
Cu	5.06 ± 2.06	21.08 ± 15.75
Zn	42.16 ± 20.13	153.71 ± 73.68
Sr	6.34 ± 1.03	8.67 ± 2.73
Zr	3.44 ± 4.22	7.03 ± 6.43
Sn	6.21 ± 7.85	7.57 ± 7.45
Sb	6.04 ± 10.64	10.06 ± 14.01
Te	17.97 ± 20.89	11.23 ± 14.77
Cs	5.06 ± 4.24	0.15 ± 0.80
Lu	7.28 ± 5.31	30.19 ± 13.58
U	67.95 ± 101.93	28.89 ± 53.82
Ni	31.12 ± 2.69	13.10 ± 9.93
Er	3.46 ± 3.14	20.66 ± 11.46
Pb	0.52 ± 1.01	9.99 ± 6.66
W	3.47 ± 3.17	9.24 ± 6.40
P	1.42 ± 2.51	22.67 ± 16.04
Br	1.80 ± 3.30	33.31 ± 72.68

Figure S2. Level of concentrated $PM_{2.5}$ in various groups and elemental composition, Related to Figure 1

Supplementary Figure 3

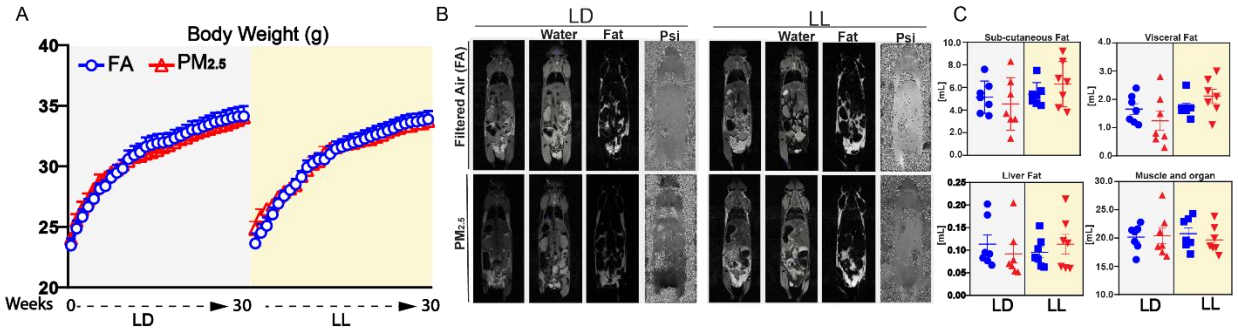

Figure S3. Impact of air-pollution ($PM_{2.5}$) and light at night (LL) on whole body fat mass, Related to Figure 1

Supplementary Figure 4

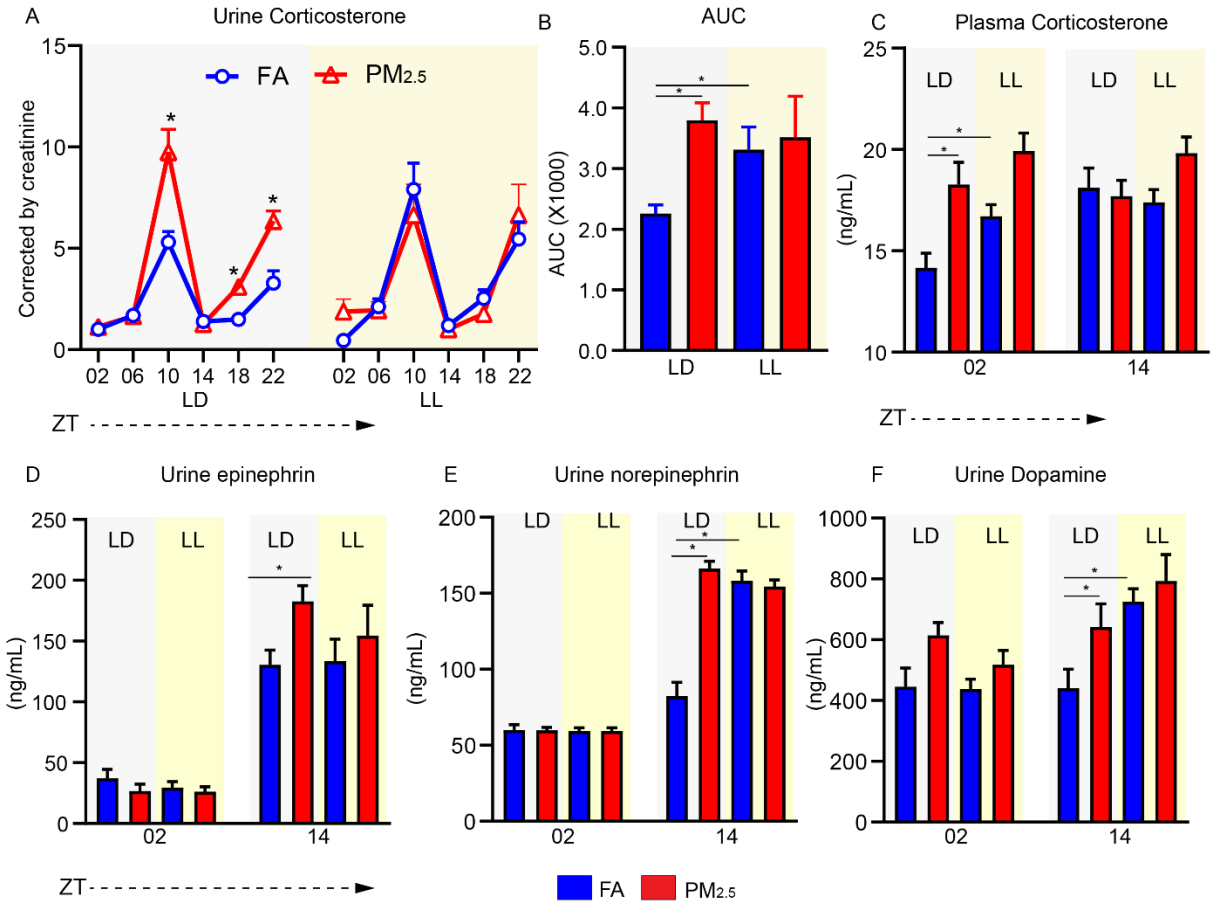

Figure S4. Effect of air-pollution ($PM_{2.5}$) and light at night (LL) on plasma and urinary catecholamine level, Related to Figure 2

Supplementary Figure 5

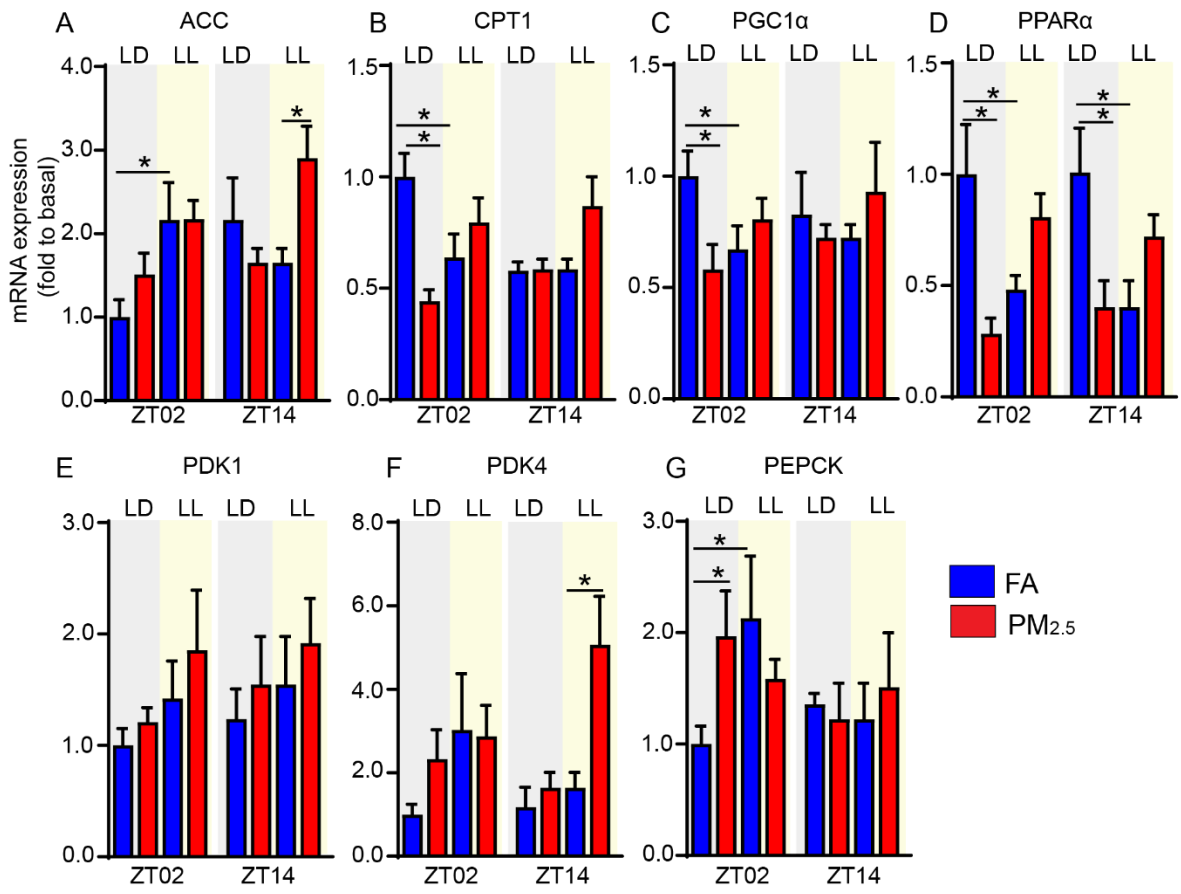

Figure S5. Expression level of metabolically active genes in liver of wild type mice exposed with air-pollution ($PM_{2.5}$) and light at night (LL), Related to Figure 2

Supplementary Figure 6

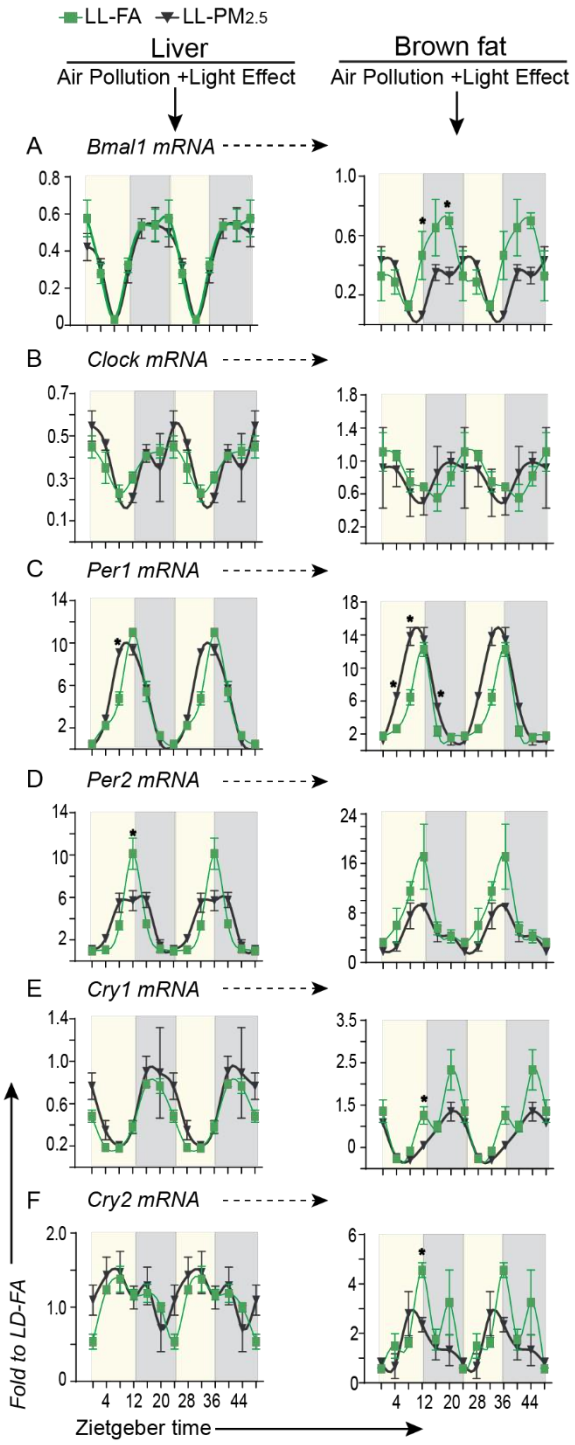

Figure S6. $PM_{2.5}$ plus Light on peripheral circadian rhythm in wild type mice, Related to Figure 2

Supplementary Figure 7

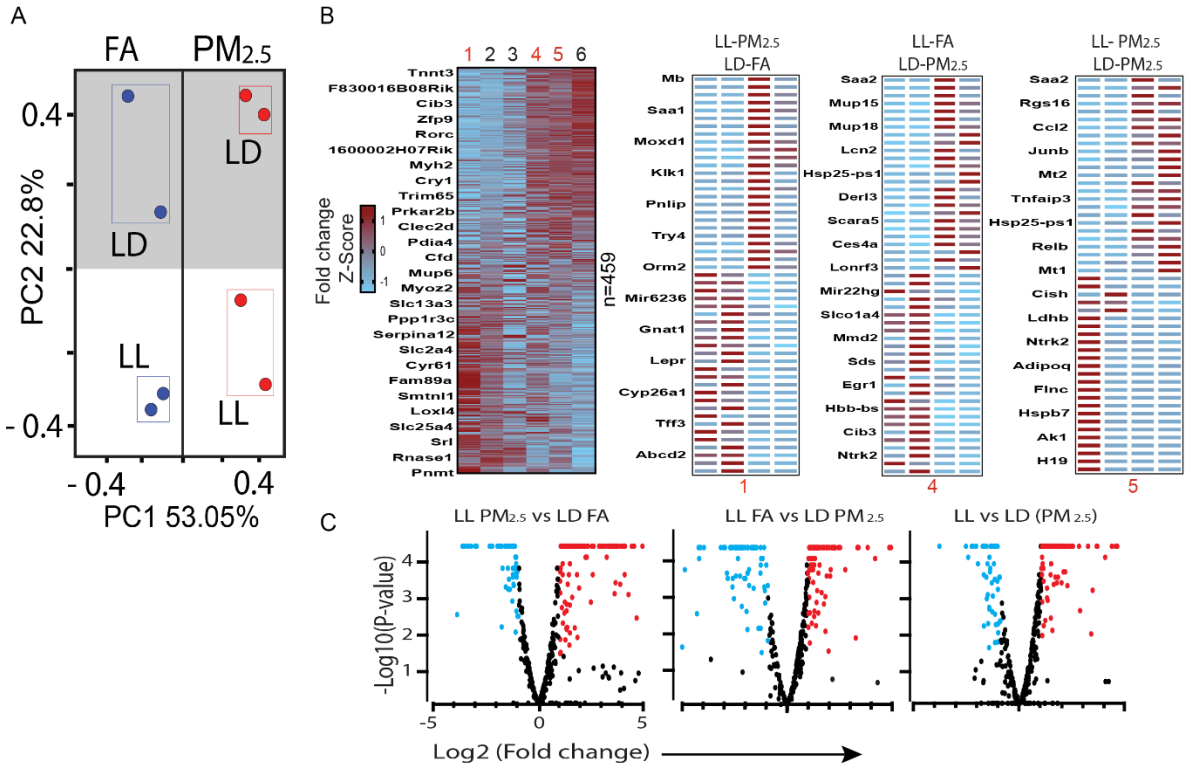

Figure S7. Differential effect of $PM_{2.5}$ and light at night (LL) on liver transcriptome, Related to Figure 3

Supplementary Table 1

Circadian gene		MESOR	p Value	Amplitude	p Value	Acrophase	p Value	Cycling p Value
Bmal1	*LD-FA*	*0.4751475*		*0.4781546*		*23.210186*		*0.00515**
	LD-PM$_{2.5}$	*0.2235200*	*1.20871e-05* [a]	*0.2572473*	*0.00045615* [a]	*20.901409*	*0.000653919* [a]	*0.00905**
	LL-FA	*0.3808750*	*0.009795208* [b]	*0.2664871*	*0.00023165* [b]	*19.996965*	*0.004202895* [b]	*0.04654**
	LL-PM$_{2.5}$	*0.3524100*	*0.279870462*	*0.2345565*	*0.49459407*	*19.997475*	*0.999582386*	*0.04404**
Clock	*LD-FA*	*0.4711575*		*0.3836382*		*22.370084*		*0.04856**
	LD-PM$_{2.5}$	*0.3396225*	*0.036872430* [a]	*0.1591120*	*0.00774965* [a]	*17.386595*	*0.407066262*	*0.17555*
	LL-FA	*0.3607225*	*0.028926914* [b]	*0.1072335*	*0.00124737* [b]	*21.179567*	*0.173478699*	*0.02633**
	LL-PM$_{2.5}$	*0.3644100*	*0.856085727*	*0.1770454*	*0.02970233* [c]	*11.621043*	*0.143700042*	*0.17720*
Per1	*LD-FA*	*4.4871700*		*4.6587179*		*12.093686*		0.21697
	LD-PM$_{2.5}$	*3.0142900*	*0.010469893* [a]	*2.6414670*	*0.00922050* [a]	*12.923761*	*0.230090565*	0.27133
	LL-FA	*4.1883250*	*0.149405844*	*4.6550357*	*0.97823434*	*11.921178*	*0.694543269*	0.05033
	LL-PM$_{2.5}$	*4.649775*	*0.081613087*	*5.1780636*	*0.23105892*	*10.791905*	*0.097955216*	0.00188*
Per2	*LD-FA*	*2.6156725*		*2.4929648*		*12.412633*		0.04938*
	LD-PM$_{2.5}$	*4.0378350*	*0.011507130* [a]	*4.6612373*	*0.03264309* [a]	*12.352367*	*0.927495226*	0.12304
	LL-FA	*3.3550250*	*0.104936630*	*3.8369929*	*0.05141281* [b]	*12.069062*	*0.582640653*	0.11987
	LL-PM$_{2.5}$	*3.5986670*	*0.553462790*	*2.9362332*	*0.19829811*	*11.920924*	*0.821233843*	0.11403
Cry1	*LD-FA*	*0.6518600*		*0.5872745*		*19.723241*		0.00709*
	LD-PM$_{2.5}$	*0.4611925*	*0.025545406* [a]	*0.1964905*	*0.00298631* [a]	*20.152340*	*0.702949206*	0.19075
	LL-FA	*0.4634350*	*0.024643128* [b]	*0.3491752*	*0.02801319* [b]	*18.386989*	*0.099875546*	0.00192*
	LL-PM$_{2.5}$	*0.5822700*	*0.124363775*	*0.4158133*	*0.70669751*	*15.154233*	*0.521417173*	0.01544*
Cry2	*LD-FA*	*1.3202800*		*0.4781722*		*13.018262*		0.03312*
	LD-PM$_{2.5}$	*1.2162175*	*0.621442695*	*0.4071473*	*0.59094435*	*8.3898884*	*0.046945202* [a]	0.39293
	LL-FA	*1.0841250*	*0.131232826*	*0.3007884*	*0.16074719*	*10.272730*	*0.023742458* [b]	0.25913
	LL-PM$_{2.5}$	*1.1878725*	*0.514822831*	*0.3606528*	*0.20918143*	*8.1397044*	*0.244456881*	0.23006

Table S1. Cosinor analysis of circadian genes in liver, Related to Figure 2

Supplementary Table 2

Circadian gene		MESOR	p Value	Amplitude	p Value	Acrophase	p Value	Cycling p Value
Bmal1	*LD-FA*	*0.5821500*		*0.6853124*		*21.530963*		0.00851*
	LD-PM$_{2.5}$	*0.3038200*	*0.002594268* [a]	*0.3031707*	*0.00510237* [a]	*22.558070*	*0.242813991*	0.03124*
	LL-FA	*0.4272600*	*0.093637845*	*0.3365980*	*0.01085447* [b]	*18.305526*	*0.094588572*	0.03367*
	LL-PM$_{2.5}$	*0.2787175*	*0.037792743* [c]	*0.1830650*	*0.03929240* [c]	*22.717388*	*0.026670530* [c]	0.12201
Clock	*LD-FA*	*0.9086000*		*0.3871367*		*21.297822*		0.04230*
	LD-PM$_{2.5}$	*0.7749100*	*0.079960450*	*0.4503129*	*0.67776922*	*16.818658*	*0.114922991*	0.07101
	LL-FA	*0.8288100*	*0.307560990*	*0.3313560*	*0.73352477*	*7.6363178*	*0.046405087* [b]	0.08610
	LL-PM$_{2.5}$	*0.7934325*	*0.828200913*	*0.4418717*	*0.34566122*	*13.517189*	*0.438437759*	0.05307
Per1	*LD-FA*	*3.2319550*		*2.8540918*		*10.970798*		0.18724
	LD-PM$_{2.5}$	*5.4244900*	*0.009184235* [a]	*6.6456521*	*0.01193468* [a]	*10.657929*	*0.473685066*	0.09304
	LL-FA	*4.4973250*	*0.026183497* [b]	*4.5341405*	*0.10478281*	*10.765168*	*0.623734731*	0.16854
	LL-PM$_{2.5}$	*6.9292800*	*0.031107098* [c]	*7.1509239*	*0.08483440*	*9.7282170*	*0.117572427*	0.00335*
Per2	*LD-FA*	*5.5682800*		*6.0155055*		*15.055741*		0.04731*
	LD-PM$_{2.5}$	*3.8727700*	*0.229019036*	*3.7949755*	*0.31544190*	*14.184400*	*0.393365511*	0.19858
	LL-FA	*7.9235450*	*0.197950379*	*6.2111323*	*0.91310225*	*10.555955*	*1.40345e-05* [b]	0.08589
	LL-PM$_{2.5}$	*4.9585725*	*0.043436820* [c]	*3.9118945*	*0.06504908*	*11.635098*	*0.417037191*	0.06571
Cry1	*LD-FA*	*1.1916275*		*1.4510653*		*19.372820*		0.03471*
	LD-PM$_{2.5}$	*0.6640700*	*0.002828390* [a]	*0.6520268*	*0.010979775* [a]	*18.309051*	*0.532259820*	0.04413*
	LL-FA	*1.0986325*	*0.508046290*	*0.8333420*	*0.029669969* [b]	*18.918508*	*0.529200260*	0.17684
	LL-PM$_{2.5}$	*0.7328075*	*0.024801920* [c]	*0.5907753*	*0.128065244*	*19.765730*	*0.236281690*	0.03133*
Cry2	*LD-FA*	*2.6129025*		*2.7754165*		*17.409901*		0.08550
	LD-PM$_{2.5}$	*1.4265425*	*0.016264978* [a]	*1.0171037*	*0.005313846* [a]	*16.856182*	*0.7858926630*	0.35483
	LL-FA	*2.2101400*	*0.320025389*	*1.4079303*	*0.030145224* [b]	*14.365625*	*0.0770324520*	0.42185
	LL-PM$_{2.5}$	*1.5626150*	*0.122093005*	*1.1280335*	*0.522138861*	*12.255406*	*0.3315054400*	0.16734

Table S2. Cosinor analysis of circadian genes in BAT, Related to Figure 2

Supplementary Table 3

Primer	Forward	Reverse
Clock	5'-GAGGTCGTCCTTCAGCAGTC -3'	5'-TGTGACATGCCTTGTGGAAT -3'
Bmal1	5'-AAGTGCAACAGGCCTTCAGT - 3'	5'-GGTGGCCAGCTTTTCAAATA -3'
Per1	5'-CCAGGATGTGGGTGTCTTCT -3'	5'-TTTCCTGGGTGAAGTCCTTG -3'
Per2	5'-ATTGGGAGGCACAAAGTCAG -3'	5'-CAGTAGCCGGTGGATTTGTT -3'
Cry1	5'-TTCACTGCTACTGCCCTGTG -3'	5'-TTTTGCAGGGAAGCCTCTTA -3'
Cry2	5'-ATGTGTTCCCAAGGCTGTTC -3'	5'-CCTCCTTGGCCATCTTCATA -3'
ACC	5'-GGATGACAGGCTTGCAGCTAT -3'	5'-TTTGTGCAACTAGGAACGTAAGTCG -3'
PDK1	5'-TCCTGTCACCAGCCAAAATG -3'	5'-CCACCGAACAATAAGGAGTGC -3'
PDK4	5'-GAGGATTACTGACCGCCTCTTTAG -3'	5'-TTCCGGGAATTGTCCATCAC -3'
PEPCK	5'-CCCTTGTCTATGAAGCCCTCA -3'	5'-GCCGAAGTTGTAGCCGAAGA -3'
PPARα	5'-ACACTGCCAAGGAGTCGAG -3'	5'-AGGCATCTACCACCATGTCCATAA -3'
PPARγ	5'-AGCTGACCCAATGGTTGCTGATTA -3'	5'-GGAGATGCAGGTTCTACTTTGATCG -3'
CPT1	5'-CTGCTGCATGGTAGATGTTTCGAC -3'	5'-GCCCAGGAATGCTCTGCGTTTA -3'
PGC1α	5'-AGCCGTGACCACTGACAACGAG -3'	5'-GCTGCATGGTTCTGAGTGCTAAG -3'
UCP1	5'-GGCATTCAGAGGCAAATCAGCT -3'	5'-CAATGAACACTGCCACACCTC -3'
PRDM16	5'-CCACCAGCGAGGACTTCAC -3'	5'-GGAGGACTCTCGTAGCTCGAA -3'
HDAC1	5'-AGTCTGTTACTACTACGACGGG' -3	5'-TGAGCAGCAAATTGTGAGTCAT -3'
HDAC2	5'-GCGTACAGTCAAGGAGGCGGC' -3	5'-GGCTTCATGGGATGACCCTGGC' -3'
HDAC3	5'-CACCAAGAGCCTTGATGCCTT' -3	5'-GCAGCTCCAGGATACCAATTACT' -3'
HDAC4	5'-TGAGAGACGGAGCAGCCCCC -3	5'-TGGAGAGCTGGGACCGGAGC -3'
DNMT1	5'-CCTAGTTCCGTGGCTACGAGGAGAA -3	5'-TCTCTCTCCTCTGCAGCCGACTCA -3'
DNMT3A	5'- GCCGAATTGTGTCTTGGTGGATGACA' -3	5'-CCTGGTGGAATGCACTGCAGAAGGA -3'
GAPDH	5'- AACGACCCCTTCATTGAC' -3	5'-TCCACGACATACTCAGCAC -3'
RPL13A	5'-GGAGAAACGGAAGGAAAAGG -3'	5'-GAGTCCGTTGGTCTTGAGGA -3'
B2M	5'-TGGTGCTTGTCTCACTGACC -3'	5'-TATGTTCGGCTTCCCATTCT -3'

Table S3. Mouse primers used for Circadian Rhythm and Metabolic Study, Related to Figure 2, Figure 5 and Fig S5 and Fig S6

Transparent Methods

Exposure of Animals to Ambient $PM_{2.5}$

Laboratory mice were exposed to concentrated ambient $PM_{2.5}$ or filtered air (FA) using a Versatile Aerosol Concentration Enrichment System (VACES) whose laboratory and field characterization have been previously described in detail (Chen, 2003) (Maciejczyk and Chen, 2005; Sun et al., 2009). VACES allows the concentration of ambient particulates in the atmosphere in Cleveland, Ohio, USA, allowing chronic inhalational exposure of mice in chambers to concentrated ambient particulate matter <2.5 microns (CAP) in diameter. Briefly, the sampled ambient aerosol from VACES located in metropolitan Cleveland is drawn inside a saturator and mixed with ultrapure deionized water vapor to achieve saturation, following which it passes through a cooling section that induces condensational growth of the particles to super-micrometer size via supersaturation. The grown particles are then concentrated by virtual impaction. VACES employs three virtual impactors in parallel, achieving an overall enrichment factor of 10-20x, depending on ambient concentration levels. The particles themselves are analyzed after collection on Teflon filters using XRF (X-ray fluorescence, a non-destructive analytical technique) analysis to determine the elemental composition of deposited $PM_{2.5}$. The elemental composition during exposure for this experiment is depicted in Supplemental Figure 2. For the initial discovery study, three-week-old C57BL/6J male mice were purchased from the Jackson Laboratories (Bar Harbor, ME), and were equilibrated for 1 week prior to experimental enrollment. Weight matched mice were then divided into two groups and exposed to either filtered air (FA) and/or concentrated $PM_{2.5}$ at nominal 10 × (80-100μg/m^3) ambient concentrations 6 hours per day, 5 days per week in standard light-dark cycle (12 h day light/12 h dark) (LD) with concomitant *ad libitum* access to standard chow diet for 14 weeks. For the validation study, three-week-old C57BL/6J male mice were equilibrated for 1

week prior to experimental enrollment and divided into four groups; (1) LD-FA (12h day light/12h dark and received filtered air daily 6h/day/5 days in a week). (2) LD-$PM_{2.5}$ (12h day light/12h dark and received concentrated $PM_{2.5}$ air daily 6h/day/5 days in a week). (3) LL-FA (12h day light/12h dim light and received filtered air daily 6h/day/5 days in a week) and (4) LL-$PM_{2.5}$ (12h day light/12h dim light and received concentrated $PM_{2.5}$ air daily 6h/day/5 days in a week) with concomitant *ad libitum* access to standard chow diet for 30 weeks. The control (FA) mice in the experiment were exposed to an identical protocol with the exception of a high-efficiency particulate-air (HEPA) filter positioned in the inlet valve position to remove all of the $PM_{2.5}$ in the filtered air stream. All the animal experiments were approved by the Case Western Reserve University IACUC committee and carried out under the institutional guidelines for ethical animal use.

Glucose and Insulin Tolerance Test

Basal blood glucose was measured after 12h of fasting using a handheld glucometer (Contour). Mice were given an intraperitoneal bolus of glucose (glucose tolerance test) or insulin (insulin tolerance test) at a concentration of 2 mg/kg or 0.75 IU/kg body weight, respectively, and blood glucose was measured at 20, 40, 60, 90 and 120 minutes thereafter.

Blood Glucose, Plasma Insulin

Retro-orbital blood was collected under isoflurane anesthesia after 12 hours of fasting. Whole-blood glucose was determined by using the glucometer (Contour) with glucose test strips as described by the manufacturer. Plasma insulin was determined by using a mouse insulin ELISA kit with mouse insulin as a standard (Alpco, Salem, NH03079). The homeostatic model assessment of insulin resistance (HOMA-IR) was calculated using the equation [(Glucose × Insulin)/405].

Urine and Plasma Corticosteroid Assay

Catecholamine levels such as epinephrine, nor-epinephrine and dopamine (3-CAT ELISA assay kit, Rocky Mountain Diagnostic Inc., Colorado Springs, CO 80903, USA) and total corticosterone level (Life Technology Corporation, Frederick, MD, USA) were measured according to the manufacturer instructions. Briefly, urine from different groups of mice were collected at ZT2, ZT6, ZT10, ZT14, ZT18, and ZT22 time points and stored at -80^{o}C or used for catecholamine and total corticosterone measurement. For plasma total corticosterone levels, blood collected at ZT2 and ZT14 was used for this assay.

***In vivo* Glucose Uptake Measured by Positron Emission Tomography**

[18F] Fluorodeoxyglucose (FDG) was purchased from PETNET solution (Cleveland, USA) and a cyclotron (Siemans20–30 gb). After an 8 h fast mice were injected with insulin (0.75 U/kg) diluted in 0.9% physiological saline and 5 min later received an intravenous administration of FDG (200-300μCi). After injection, the mice were maintained under conscious conditions and warmed using a heating pad. Before PET imaging, a CT scout view was taken to ensure mice were placed in the co-scan field of view (FOV) where the highest image resolution and sensitivity are achieved. Once the static acquisition was done, a CT acquisition scan was performed for attenuation correction. At 30 min small-animal positron emission tomography (uPET/CT, Siemens Medical solution Inc, TN 37932, USA) and micro-computed tomography (CT) (uPET/CT: Inveon, Siemens Medical solution Inc, TN 37932, USA) imaging were performed using an acquisition time of 15-30 min for PET at Case Center for Imaging Research (CCIR). Quantitative image analysis of the uptake of ^{18}F-FDG in different organs was performed using Carimas II software. This program allows the regions of interest (ROI) to be extrapolated from the reconstructed uPET image frames, allowing the quantification of the SUV (standard uptake value) in a specific region. Based on the PET and

CT co-registered images, brain, liver, heart, muscle, WAT and BAT were then defined as (ROI) and FDG tissue uptake calculated using the mean value of standard uptake values (SUV).

Body Composition and Indirect Calorimetry

In vivo body composition analysis of lean mass and fat mass from conscious, immobilized mice was performed by the Case Center for Imaging Research (CCIR). The data and images were collected as described previously (Johnson et al., 2012) by using Bruker Biospec 7T small animal MRI scanner (Bruker Biospin, Billerica, MA). For indirect *in vivo* metabolic analyses, 20 weeks of FA/$PM_{2.5}$-exposured mice were acclimated to the apparatus for 24 hours before data collection commenced, after which energy expenditure was measured using a computer-controlled indirect calorimetry system (Oxymax Comprehensive Lab Animal Monitoring System, Columbus Instruments, Columbus, OH), run by the MMPC (Mouse Metabolic Phenotyping Core) at Case Western Reserve University (CWRU). For each animal, O_2 consumption and CO_2 production were measured for 1 min at 10-min intervals. Respiratory Quotient (RQ) was calculated as the ratio of CO_2 production to O_2 consumption. Energy expenditure was calculated using the Weir equation with normalization to body weight. Light and dark cycle energy expenditure was determined using the average of all data points per 12-h light/dark cycle of 2 consecutive days, and these, in turn, were averaged to obtain total 24-h energy expenditure. Data acquisition and instrument control were coordinated by MetaScreen and raw data was processed using ExpeData with an analysis script documenting all aspects of data transformation.

Quantitative Real-Time RT-PCR (qPCR) Analysis

Total RNA was extracted from liver and brown fat using Trizol® Reagent (Life Technologies, Grand Island, NY). cDNA was synthesized using Transcriptor First Strand cDNA synthesis kit (Roche Applied Science, Indianapolis, IN) according to the manufacturer's protocol. The

amplification of target genes was used by a LightCycler® 480 SYBR Green I Master kit (Roche Applied Science, Indianapolis, IN). Gene expression was measured by quantitative real-time PCR performed on a LightCycler® 480 real-time PCR System (Roche Applied Science, Indianapolis, IN). The sequences of real-time PCR primers used in this study are shown in Supplementary Table 3. Fold changes of mRNA levels were determined using the ΔΔCt method and normalized to internal control GAPDH, RPL13 and B2M.

RNA-Sequencing

The extracted RNA was quantified by NanoDrop (Thermo Fisher Scientific, MA) and the quality was assessed using a 2100 Bioanalyzer (Agilent Technologies, CA). The Agilent Bioanalyzer is a microfluidics platform used for sizing, quantification, and quality control for RNA (and DNA/ proteins) and provides an "RNA Integrity Number" (RIN), which quantifies the fragmentation of the RNA sample. The RNA samples were selected for sequencing if RIN value was more than 6.5. On average, 500-1,000 mg of RNA samples were used for library preparation and double-stranded cDNA generation. We utilized the NEBNext® Ultra RNA Library Prep Kit (New England BioLabs, Inc, Ipswich, MA) for liver tissues and a TrueSeq RNA Library Prep Kit (Illumina, San Diego, CA) to generate strand-specific libraries for all other mentioned issues. The library was amplified by 15-cycle according to the manufacturer protocol. After PCR primers removal with Agencourt AMPure PCR purification kit (Beckman Coulter, CA), the sequencing library was quantified on TapeStation (TapeStation Instrument). The prepared library was sequenced by HiSeq series sequencer including HiSeq4000, HiSeqX (Illumina, San Diego, CA). The raw BCL files were converted into FastQ files using CASAVA 1.8.2 (CASAVA).

Transcriptome Analysis

A total of 500 million reads were used, with an average of 50 million reads per sample. We built an index sequence for STAR using the Gencode M13 reference feature that includes protein-coding genes as well as non-coding genes. In total, 50,600 genes and 124,031 transcripts including isoforms were identified. Prior to sequence alignment, we applied trimgalore (version 0.4.3) with cut adapt package (version 1.12) (Martin, 2011) for removing any unnecessary genomic fragments (e.g. adapter dimers) and low quality nucleotide sequences from the raw reads. We mapped raw sequencing reads to the mouse reference genome (mm10) using STAR aligner 7, and calculated the raw count using feature Counts package (Risso et al., 2014). Finally, we extracted gene level transcripts (N=50,600) and transcript level isoforms (N=124,031) using the feature Counts. To test reproducibility and examine outlier samples, we conducted PCA analysis and MDR block analysis, as well as pair-wise comparative analysis showing the correlation scores in a matrix format (Fig. S1). We excluded extreme outlier samples before conducting differentially expressed gene analysis. All datasets are deposited under GEO accession number (GSE145566) and are accessible to the scientific community.

Differentially Expressed Genes (DEGs)

We used protein coding genes and long non-coding RNA from Gencode M13 (Freeze date Oct 2016). For transcriptome analysis, we were primarily interested in assaying gene-level expression (protein-coding genes). We used Rsub read and feature counts to generate a gene-by-sample matrix of reading counts that was analyzed using edgeR after removing unwanted variation (RUVg) (Risso et al., 2014). The output of this analysis is a set of genomic regions that are significantly different between the experimental groups. For transcript level expression analysis, we also utilized the alignment free mapping method in Salmon to quantify the number of transcripts and

transcript per million (TPM). We compared gene-level DEGs and transcript level DEGs and summarized the results in Supplementary Table 4. Due to the small number of biological replicates (N=2), we utilized the limma based edgeR method to determine differentially expressed transcripts or isoforms; cutoff: log2FC > 0.7 for liver and adipose samples (log CPM>0.7, FDR < 0.05). We used a low threshold in fold change (low-fold change DEGs: log2FC between 0.7 and 1.0) due to the potentially small effect size of environmental exposure on epigenome or transcription, resulting in only small variations in the transcriptome. We performed GO and Pathway analysis using DEGs and control genes. We used R Package Top GO 9 to generate the GO and GSEA to generate KEGG/Reactome pathways. In addition, we performed IPA (Ingenuity Systems Inc., Redwood City, CA) to check for enriched pathways from DEGs and search for upstream regulators (TF, enzyme, receptors). To validate our findings Transfac, and HOMER analysis 10 were performed to confirm upstream regulators from the DEGs list.

Open Chromatin Signatures from Liver Samples using ATAC-seq

Livers from 14-week-exposed male mice were harvested and the left lobe of liver was pulverized. Using same Freezer Mill (6775 Freezer/Mill® Cryogenic Grinder) that was used in RNA-seq library prep, 20-30 mg of frozen liver powder was used for prepare ATAC-seq library. The OMNI ATAC-seq protocol (Corces et al., 2017) was adopted for isolating nuclei and applying transposase reaction. The library was purified using two-sided SPRI beads selection (100-500bp fragment size). We utilized Hi-Seq system to sequence the libraries. Due to the limitation of the original protocol, we have relatively high background noise (compare to the advanced OMNI ATAC-seq protocol) (Martin, 2011) and less number of reads under the predicted peaks (open chromatin). Briefly, all reads were trimmed using cut adapt package, and trimmed read (>36bp minimum alignment length) have been mapped against mm10 genome using BWA aligner (Li and Durbin,

2009). The candidate peaks were predicted by MACS peak calling software (Zhang et al., 2008). Parameters used for open chromatin peaks (-g mm -q 0.01 –keep-dup 1000 –no model –shift 0 -extsize 150), fine grain and smaller peaks (-extsize 40). We used predicted open chromatin peaks where at least two biological replicates were reproducible for the downstream analysis using IDR cutoff 0.05.(Q Li, 2011) All the pipeline is freely available via git hub and docker image developed by Bo Zhang lab at WASHU (https://hub.docker.com/r/zhanglab/atac-seq/). Finally, the open chromatin regions were submitted to search potential transcription factor binding sites using HOMER (Heinz et al., 2010) software (mm10 -size 150 -len 11). We collected high-confidence candidate motifs (p-value < 1e-10) using Homer known motif search.

ChIP-qPCR Assay

Mice liver were collected as described in the previous section, livers from two mice from each group (LD-FA, LD-$PM_{2.5}$, LL-FA, LL-$PM_{2.5}$) were used to prepare chromatin. Briefly, liver tissues (10-15mg) were fixed with 1% formaldehyde at room temperature for 15 min with swirling and quenched with 0.125M glycine for 5 min at room temperature. Cross-linked tissues were lysed in high salt buffer for 15 min in ice and subsequently nuclear lysis with SDS for 10 min in ice. Nuclear lysed extracts were subjected to sonication 30s on and 30s off using Diagenode Pico for 20-30 cycles at 4^{o}C. After sonication DNA fragment size was checked in aliquots of sonicated extract, after protease treatment and reverse crosslinking at 65^{0} C overnight. For each ChIP, 3-5ug of ChIP grade antibodies such as Bmal1 Ab3350, Clock Ab3517, p300 sc48343, pCAFsc8999 and Pol-II Millipore 05-623B were used, blocked with BSA and cross-linked on magnetic protein A/G based on the antibody of origin, at 4^{o}C for 4hr. After sonication, the lysate was checked with desirable DNA fragment size (200-800bp) and incubated with the antibody at 4^{o}C overnight. The ChIP complex was pulled down using a magnetic separator and washed with high sucrose buffer, high

salt buffer, LiCl buffer with protease inhibitor and with a final Tris wash. The immune complex was eluted and reverse cross-linked at 65^0 overnight, phenolysed and ethanol precipitated. DNA amount was quantified using qubit and the immune precipitate is quantified with no antibody as control using qPCR and desired primer for Per1 and Per2 (Supplementary Table3).

Statistics

Unless otherwise noted, values presented are expressed as means ± SEM. Statistical analyses were performed using student t-test, one- and two-way analysis of variance (ANOVA) using SAS 9.4 statistical programming. Significance was set at $P < 0.05$. The Cosinor method was used to investigate the presence of a daily 24 h rhythm. The method consists of adjusting a cosine curve to the actual 24 h time series (Cosinor method). The null hypothesis tested was that of zero amplitude, that is, no rhythmicity at the assumed frequency (24 h). A significant periodic fit was considered when the *P* value was <0.05.

References

Chen, L.C., Zhong, M. Narciso, S.P., M. Kleinman, M., C. Nadziejko, C., and Lippmann, M. (2003). Methods for Exposing Rodents and Cells to Concentrated Ambient PM using a VACES. In American Association for Aerosol Research - Particulate Matter Conference (Pittsburgh, PA.).

Corces, M.R., Trevino, A.E., Hamilton, E.G., Greenside, P.G., Sinnott-Armstrong, N.A., Vesuna, S., Satpathy, A.T., Rubin, A.J., Montine, K.S., Wu, B., et al. (2017). An improved ATAC-seq protocol reduces background and enables interrogation of frozen tissues. Nat. Methods *14*, 959-962.

Heinz, S., Benner, C., Spann, N., Bertolino, E., Lin, Y.C., Laslo, P., Cheng, J.X., Murre, C., Singh, H., and Glass, C.K. (2010). Simple combinations of lineage-determining transcription factors

prime cis-regulatory elements required for macrophage and B cell identities. Molecular cell *38*, 576-589.

Johnson, D.H., Narayan, S., Wilson, D.L., and Flask, C.A. (2012). Body composition analysis of obesity and hepatic steatosis in mice by relaxation compensated fat fraction (RCFF) MRI. J. Magn Reson. Imaging *35*, 837-843.

Li, H., and Durbin, R. (2009). Fast and accurate short read alignment with Burrows-Wheeler transform. Bioinformatics *25*, 1754-1760.

Maciejczyk, P., and Chen, L.C. (2005). Effects of subchronic exposures to concentrated ambient particles (CAPs) in mice. VIII. Source-related daily variations in in vitro responses to CAPs. Inhal. Toxicol *17*, 243-253.

Martin, M. (2011). Cutadapt Removes Adapter Sequences From High-Throughput Sequencing Reads. EMBnet.journal *17*.

Q Li, J.B., H Huang, PJ Bickel (2011). Measuring reproducibility of high-throughput experiments. Ann. Appl. Stat *5*, 1752-1779.

Risso, D., Ngai, J., Speed, T.P., and Dudoit, S. (2014). Normalization of RNA-seq data using factor analysis of control genes or samples. Nat. Biotechnol *32*, 896-902.

Sun, Q., Yue, P., Deiuliis, J.A., Lumeng, C.N., Kampfrath, T., Mikolaj, M.B., Cai, Y., Ostrowski, M.C., Lu, B., Parthasarathy, S., et al. (2009). Ambient air pollution exaggerates adipose inflammation and insulin resistance in a mouse model of diet-induced obesity. Circulation *119*, 538-546.

Zhang, Y., Liu, T., Meyer, C.A., Eeckhoute, J., Johnson, D.S., Bernstein, B.E., Nusbaum, C., Myers, R.M., Brown, M., Li, W., et al. (2008). Model-based analysis of ChIP-Seq (MACS). Genome Biol *9*, R137.